

Figure S1. Expression of *Setd7* in the endoderm and developing pancreas is conserved across vertebrate species. (A) Expression level of *setd7* in *Xenopus* embryos at indicated stages. A progressive increase in *setd7* transcript levels is measured at neurula and tadpole stages. Data were normalized to that of *odc* and represented as fold changes compared with gastrula stage sample (set to 1). Error bars represent \pm SEM. * $P < 0.05$. (B) Expression level of *Setd7* in the mouse foregut endoderm (E8.5) and pancreatic rudiments at indicated stages. Data were normalized to that of *Sdha* and represented as fold changes compared with E8.5 (set to 1). (C, D) Whole mount *in situ* hybridization (ISH) for *setd7* in gastrula (st. 10+) and neurula stage (st. 14) *Xenopus* embryos. In C, yellow arrowheads indicate *setd7* transcript in the dorsal cells adjacent to the lip. In D, hemisected st. 14 embryo shows expression of *setd7* in the anterior ventral endoderm and middle dorsal portion of the archenteron roof (see yellow open arrowheads). Both regions of the endoderm are fated to give rise to pancreas. (E) Whole mount ISH analysis for *foxa2* in hemisected neurula stage *Xenopus* embryos. *foxa2* expression partially overlaps with *setd7* in the endoderm. (F-H) Immunofluorescence analysis of *Setd7*, *Pdx1*, *Lamp1* and *GM130* in E12.5 mouse pancreas. Arrows indicate cytoplasmic *Setd7* and *GM130*. Size bar, 50 μ m. (G) Immunofluorescence analysis of *Setd7*, *Pdx1*, and *Insulin* in E17.5 mouse pancreas. Dotted circles demarcate acinar clusters negative for *Setd7*. Size bar, 50 μ m. Abbreviations, E-cadherin, E-cad; Hoechst, Hoe; *Insulin*, Ins.

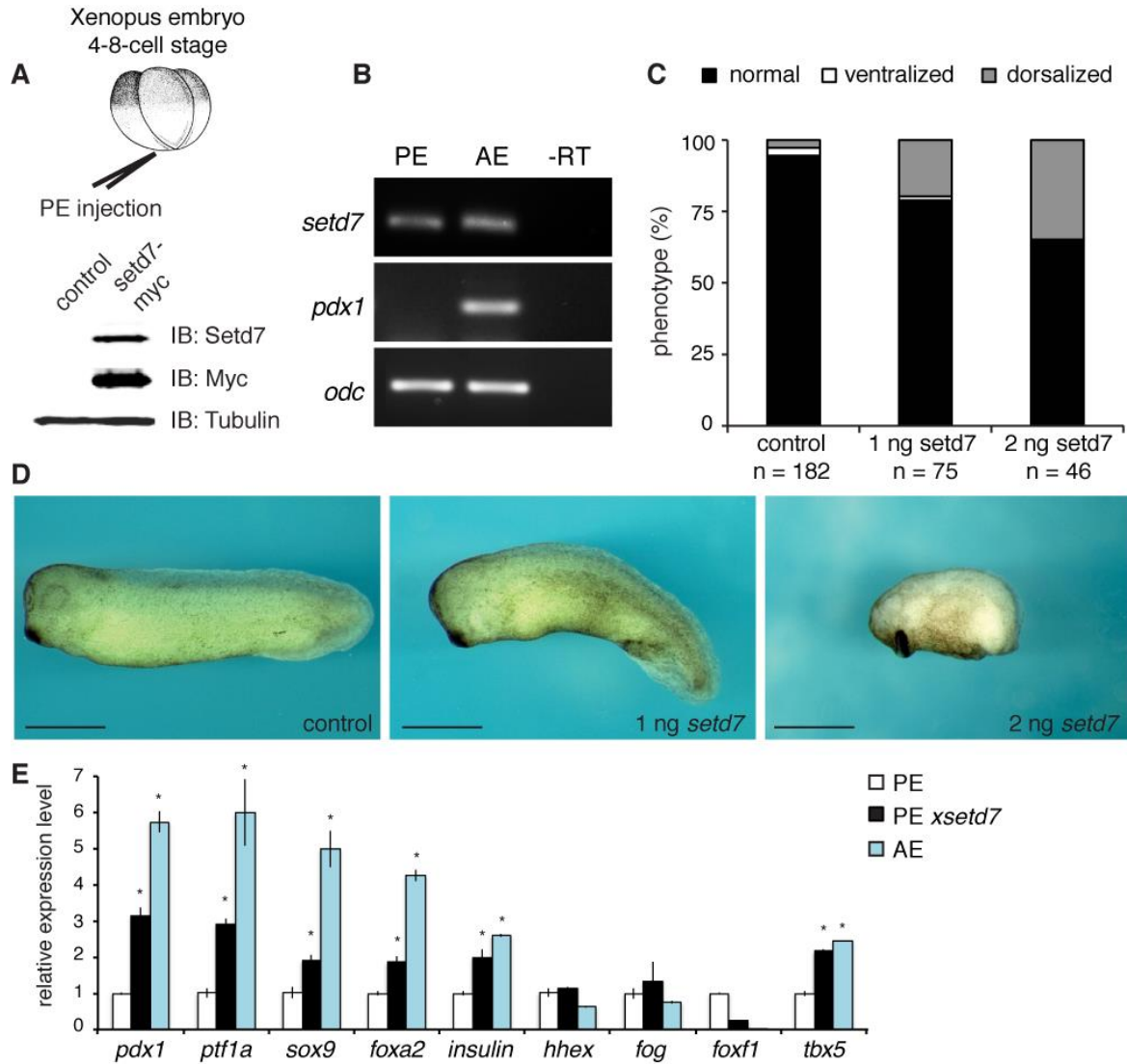


Figure S2. *Setd7* is sufficient for the specification of pancreatic progenitor cells. (A) Schematic illustration of posterior endoderm (PE) injection into 4-cell stage *Xenopus* embryos. Injection of *setd7-myc* mRNA was confirmed by Western Blot analysis. The antibody against *Setd7* does not recognize endogenous *Setd7* protein in *Xenopus* embryo extracts. (B) Semiquantitative RT-PCR of PE and anterior endoderm (AE) explants at tadpole stage (st. 28). Expression of *pdx1* is detected exclusively in AE explants, while *setd7* is expressed in both regions of the endoderm, though at higher levels in AE. (C-D) Phenotypic analysis of *setd7*-injected *Xenopus* embryos. *Setd7*-injected embryos showed slight dorsalization in a dose-dependent manner. (E) RT-qPCR analysis of indicated genes in *Xenopus* PE explants injected with *setd7* mRNA (1 ng), uninjected PE and AE. Embryos were injected into PE region at 2-4 cell st., dissected at early gastrula st., cultured until early tadpole st. and assayed for indicated genes. Data were normalized to that of *odc* and represented as fold changes compared to uninjected PE sample (set to 1). Error bars represent \pm SEM. * $P < 0.05$.

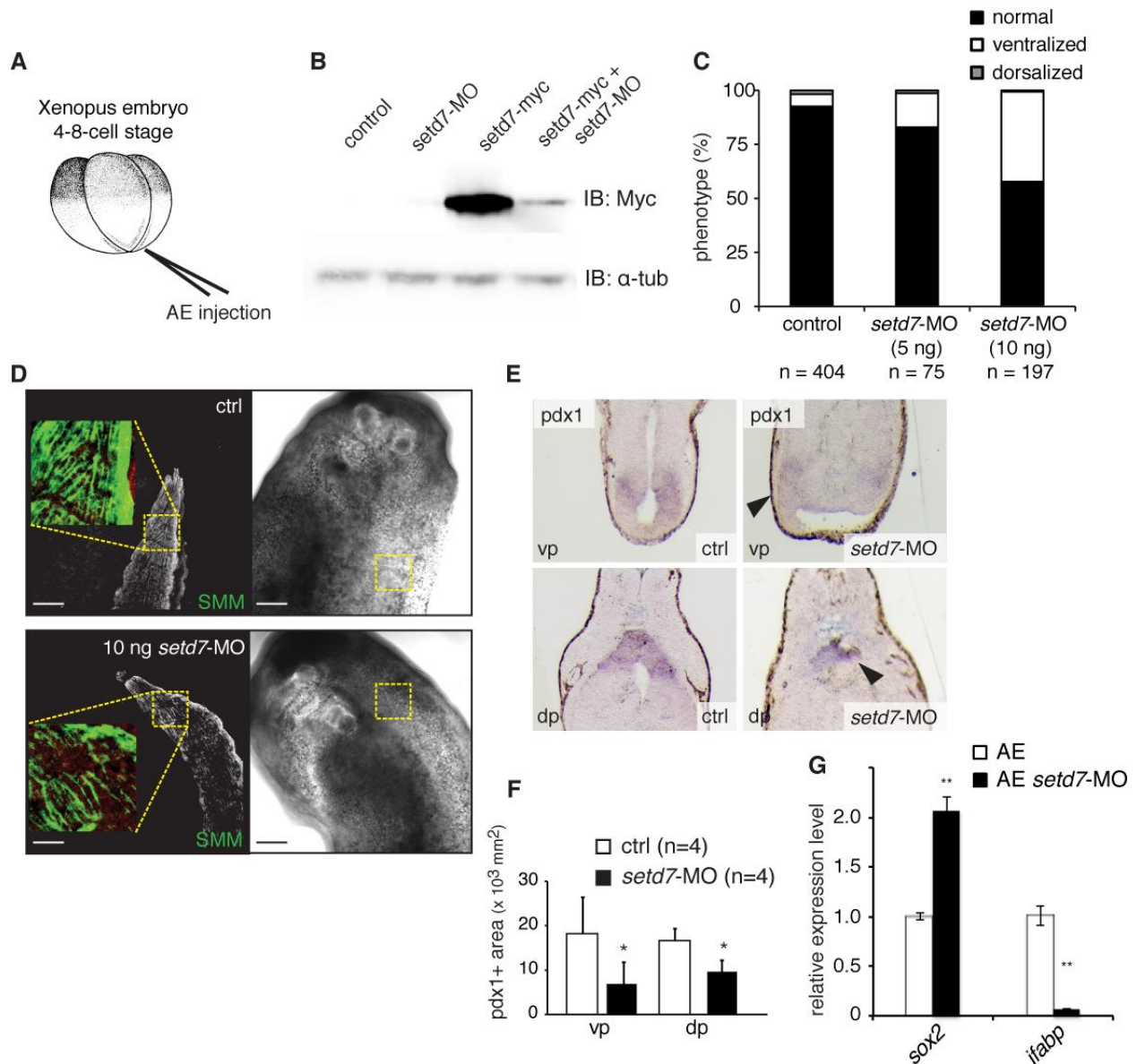


Figure S3. Setd7-MO knockdown approach in *Xenopus* embryos. (A) Schematic illustration of anterior endoderm (AE) injection into 4-cell stage *Xenopus* embryos. (B) Western blot analysis shows reduction of Setd7-myc protein in the presence of setd7-MO in *Xenopus* embryonic lysates, confirming the functionality of the designed morpholino oligonucleotide. (C) Setd7-MO-injected embryos showed slight ventralization in a dose-dependent manner. (D) Immunofluorescence analysis of skeletal muscle marker (SMM) showed disrupted muscle fibers in tadpole stage *Xenopus* embryos, which is consistent with the phenotype previously reported upon setd7-knockdown in zebrafish embryos (Tao et al., 2011). (E) *Pdx1* expression shown in transverse section of control (ctrl) and setd7-MO-injected *Xenopus* embryos processed by whole mount ISH for *pdx1*. Arrowheads indicate ventral (vp) and dorsal (dp) pancreatic buds in setd7-MO-injected embryos. (F) Quantification of the *pdx1*+ expression area in the ventral and dorsal pancreatic rudiments on transverse sections of control and setd7-MO injected *Xenopus* embryos (n=4). Error bars represent \pm SD. *P < 0.05. (G) RT-qPCR analysis of *sox2* and *ifabp* expression in *Xenopus* AE-explants injected with setd7-MO (10 ng). Data were normalized to that of *odc* and represented as fold changes compared with AE samples (set to 1). Error bars represent \pm SEM. ** P < 0.01.

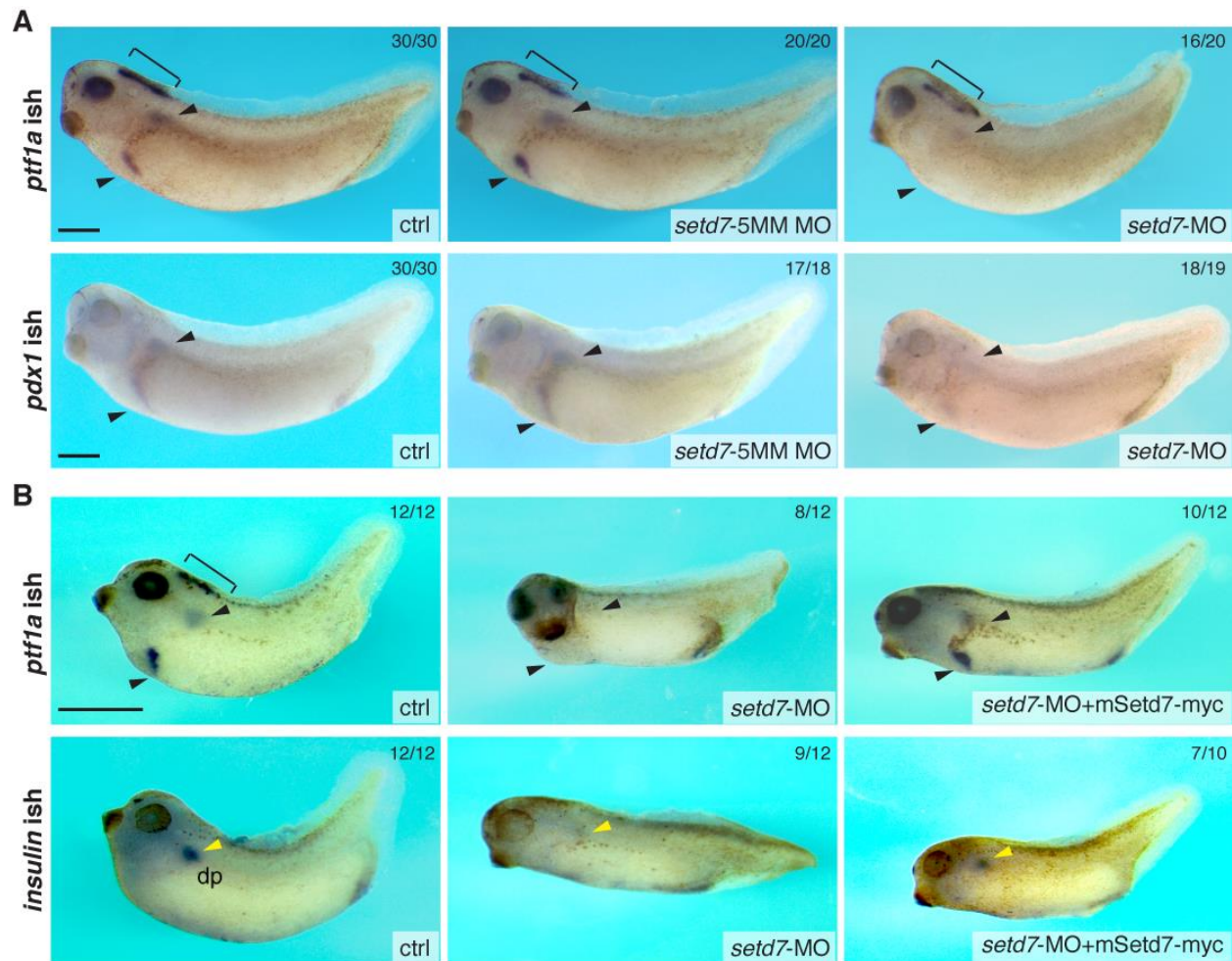


Figure S4. Control experiments for *setd7*-MO knockdown approach in *Xenopus* embryos.

(A) Whole mount ISH analysis of *ptf1a* and *pdx1* in uninjected (ctrl), 5bp-mismatched *setd7* morpholino oligonucleotide (*setd7*-5MM MO)-injected (5 ng) and *setd7*-MO-injected (5 ng) *Xenopus* embryos. A 5bp-mismatched *setd7* MO was designed introducing 5 G to C or C to G substitutions distributed evenly through the sequence and used as additional specificity control in the knockdown experiments (Eisen, Smith, 2008) (see Material and Methods for the sequences). While injection of 5 ng of *setd7*-MO led to strong reduction of pancreatic genes, the equivalent dose of *setd7*-5MM MO did not perturb pancreas formation, providing further evidence of morpholino specificity. Arrowheads indicate dorsal and ventral pancreatic buds. Brackets indicate *ptf1a* expression in the eye and hindbrain. Size bar, 1mm. n=3. (B) Whole mount ISH analysis using *ptf1a* and *insulin* antisense probes. Tadpole embryos (st. 36) injected with *setd7*-MO showed reduction of *ptf1a* and *insulin* expression domains (see arrowheads; 70%). *ptf1a* and *insulin* expression was rescued in embryos injected with *setd7*-MO and mouse *Setd7* (500 pg) mRNA (~70-80%). Embryos left untreated (ctrl) show normal *ptf1a* expression in both pancreatic buds, as indicated by the arrowheads, and hindbrain (white bracket), as well as *insulin* expression in the dp (yellow arrowheads). n=3.

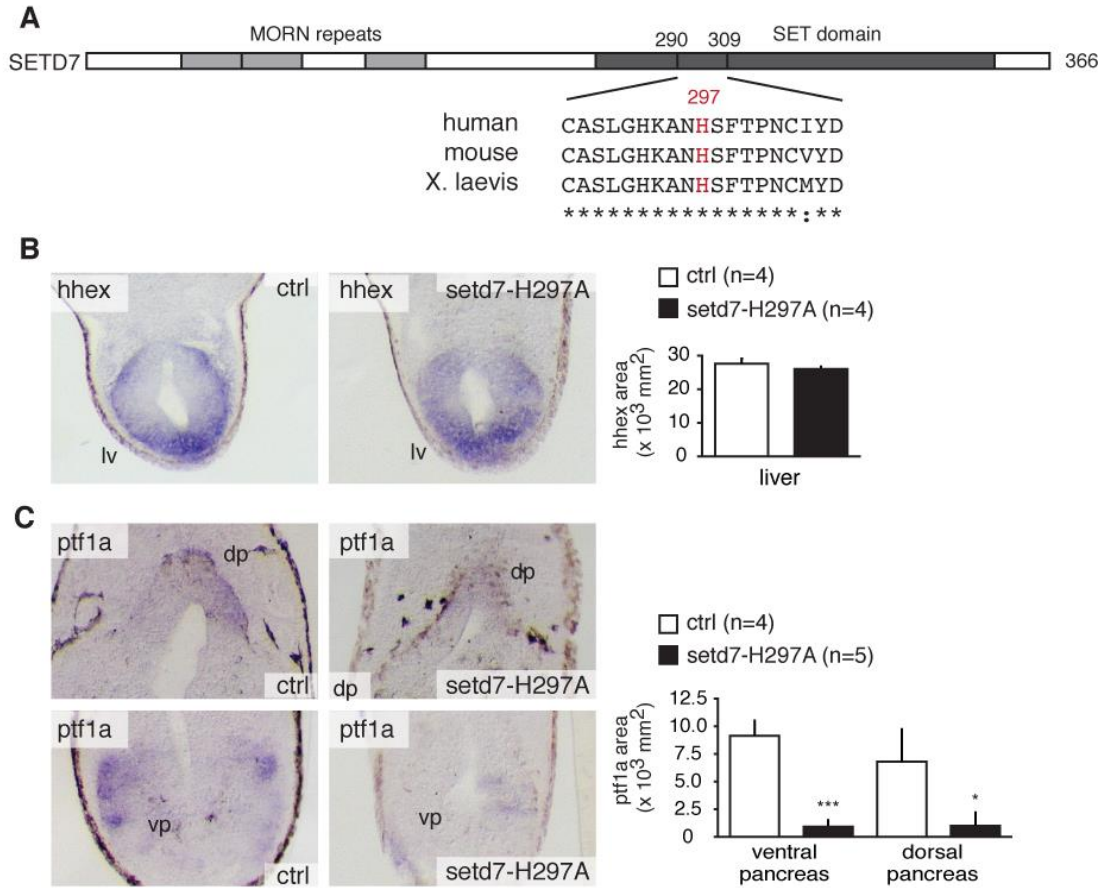


Figure S5. Activity of Setd7-H297A mutant in *Xenopus* embryos. (A) Schematic of Setd7 protein structure and amino acid alignment of the highly conserved region in the SET domain (288-306), harboring the histonemethyltransferase activity of SET proteins (Nishioka et al., 2002). The SET7 domain is highly conserved across vertebrate species, with 81% identity between the human and *Xenopus laevis* homologues. In Red, the key conserved histidine residue within the SET domain; its single amino acid substitution (H297A) results in the loss of methyltransferase activity (Nishioka et al., 2002). *Xenopus setd7-H297A* was generated by site-directed mutagenesis PCR. (B-C) *Xenopus* embryos injected with *setd7-H297A* mRNA recapitulate the same pancreatic phenotype observed in *setd7*-MO-injected embryos. Transverse sections of control (ctrl) and *setd7-H297A*-injected *Xenopus* embryos processed by whole mount ISH for *hhx* (B) and *ptf1a* (C). *Hhex*⁺ and *ptf1a*⁺ expression areas were quantified on transverse sections. Error bars represent \pm SD. *P < 0.05, **P < 0.01, ***P < 0.001. Abbreviations, dp, dorsal pancreas; vp, ventral pancreas; lv, liver.

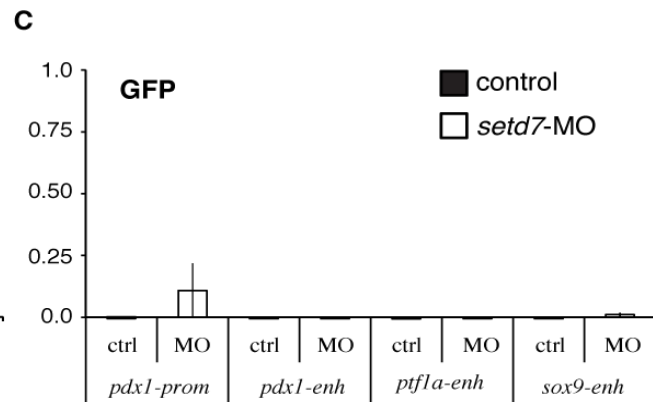
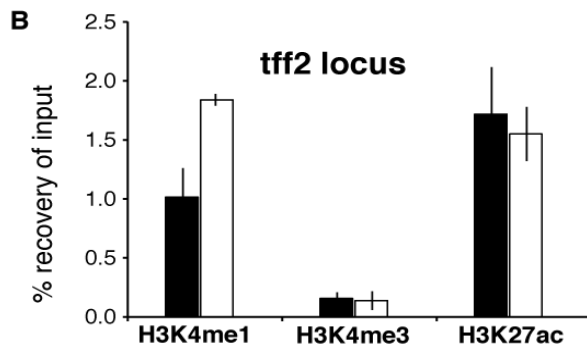
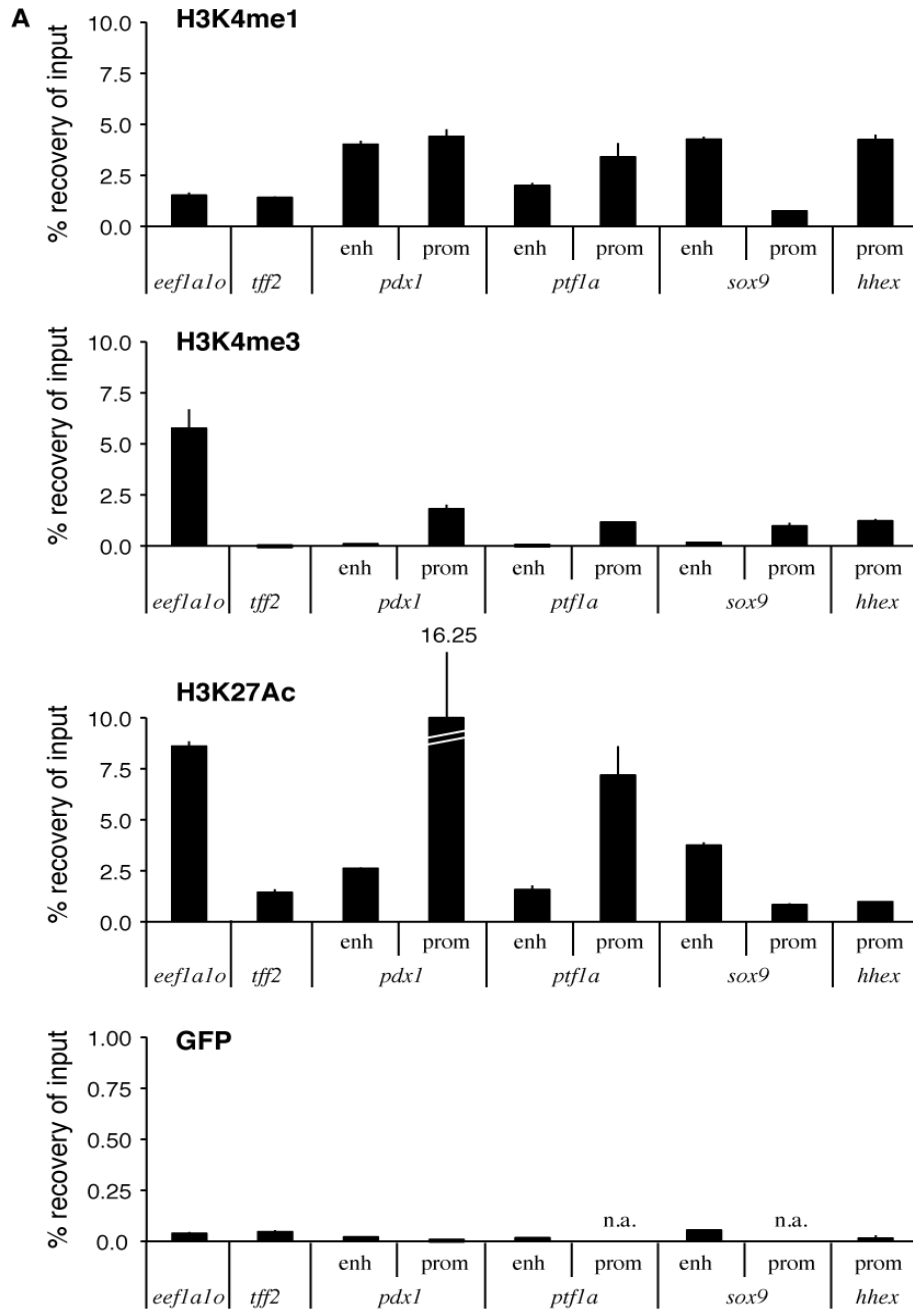


Figure S6. ChIP-qPCR control experiments. (A) ChIP-qPCR analysis of H3K4me1, H3K4me3, H3K27ac and GFP at the indicated regulatory regions in *Xenopus* embryos at tadpole stage. *Eef1a1o* (eukaryotic translation elongation factor 1 alpha 1, promoter) and *tff2* (trefoil factor 2) loci were chosen as positive and negative controls primers for H3K4me3 binding, respectively (Akkers et al., 2012). Data were normalized to % of input (*y* axis). Error bars represent \pm SD. **P* < 0.05, ***P* < 0.01, ****P* < 0.001. (B) Occupancy of H3K4me1, H3K4me3 and H3K27ac at the *tff2* locus, used as negative control locus, in control and *setd7*-MO-injected embryos. No changes in non-specific enrichment at the negative control locus were detected in *setd7*-MO-injected embryos when compared to controls. (C) ChIP-qPCR analysis of GFP at the indicated regulatory regions in control and *setd7*-MO-injected embryos at tadpole stage. As expected, GFP binding was not detected at any of the regions tested by ChIP assays. ChIP-qPCR signals were calculated as percentage of input as previously described (Blythe et al. 2009; Akkers et al., 2012; Kartikasari et al., 2013).

Table S1. Primer sequencesRT-qPCR primers (*Xenopus laevis*)

Gene	Accession number	Sequence
fog	GU384581.1	F - CAC CTC CTT TTT GTG CCA GTG R - TAT GCC CAG AAG TTA CAG GAA
for1	AF456451.1	F - TTT CCA TCT GTA GAG CCA CAA R - CTT AAT GTG ACT GAA GCA GAG
foxa2	NM_001172158.1	F - TAC CAA CAT CAA CTC CAT GAG C R - GTA ACT TCG CCG GTA AGT TTT G
foxf1	NM_001090793.1	F - AAC CCT CTG TCC TCC AGC CT R - GGT TAG TGC AAT GAC TAA CTT C
hhex	NM_001085590.1	F - CCT TTC CGC TTG TGC AGA GG R - AAC AGC GCA TCT AAT GGG AC
hnf1a	NM_001101744.1	F - CCA TGG CAA AAC TTA TGG ATT TAG A R - GGA GAT GGG GTA CTC TGA CTG
hnf1b	NM_001089811.1	F - GAA GAA AGA GAA GCT TTA GTG G R - GAC TAT ATC TCA GCC CTT GC
insulin	NM_001085882.1	F - GGC TCT ATG GAT GCA GTG TC R - GAG ACC CAC ACA AGT GCT GG
ngn3	NM_001134785.1	F - GTC TCC CAA GAG TGA CTG CC R - GAG AGA GAG GGG AGA CCT CG
odc	NM_001086698.1	F - GCC ATT GTG AAG ACT CTC TCC AAT C R - TTC GGG TGA TTC CTT GCC AC
pdx1	X16849.1	F - GTT CCC TCA GCT GCT TAT CG R - TAC CAA GGG GTT GCT GTA GG
prox1	NM_001090703.1	F - CTG ATA TCT CAC CTT ATT CGG R - TGG GAG GTG ATG CAT CTG TTG
ptf1a	NM_001174020.1	F - ATG GAA ACG GTC CTG GAG CA R - GAG GAT GAG AAG GAG AAG TTG
setd7	KX495235	F - ATG GAC AGC GAG GAT GAA ACA GTG G R - CCT TCC AAT GTG CTT CCA TCA AAA AAG
sox9	NM_001090807.1	F - CAA CTA ATT GCG CAC TGG GG R - TCT TCA GCA AAG GCA CCC AA
tbx5	NM_001085701.1	F - GCC TGC ATG TAT GCT AGT TC R - GCC TGA TGA GAA GAC TGA TG

RT-qPCR primers (Mouse)

Gene	Accession number	Sequence
Foxa2	NM_001291065.1	F - CAT CCG ACT GGA GCA GCT A R - GCG CCC ACA TAG GAT GAC
Nanog	NM_028016.3	F - CCT CCA GCA GAT GCA AGA A R - GCT TGC ACT TCA TCC TTT GG
Oct4	NM_013633.3	F - GTT GGA GAA GGT GGA ACC AA R - CTC CTT CTG CAG GGC TTT C
Pdx1	NM_008814.3	F - CCACCAAAGCTCACGCGTGGA R - GGCGGGGCCGGGAGATGTATT
Sdha	NM_023281.1	F - TGT TCA GTT CCA CCC CAC A R - TCT CCA CGA CAC CCT TCT GT
Setd7	NM_080793.5	F - CAG CCG CCA TGG ATA GCG ACG R - CTC CAG GGT GCT GCC GTC AAA G

ChIP-qPCR primers (*Xenopus*)

Gene	Sequence	Source
hhex-prom	F-CTCCAGTGCCGATTTACCTATAGAC R-CCTAAGCAACAACCTCTAGCATCA	(Rankin et al., 2011)
pdx1-enh	F-GTTCCTTTAATTCAGAGCTTTTGGG R - CCTCCATCTGGTCCAATCGC	(Boyer et al., 2006; Gao et al., 2008; Gerrish et al., 2004; Wu et al., 1997)
pdx1-prom	F - CTCAGGCTGGTAAATCAGTGA R - ATATTGTGCCATTAGGCAATTGC	(Gupta et al., 2014; Karpinka et al., 2015)
ptf1a-enh	F - GCAGGGTGGCATGATGAATG R - CCGGCTTTGTTCTGCCTGA	(Karpinka et al., 2015; Pashos et al., 2013)
ptf1a-prom	F - GCCTCCCCACAACCTCGCTGG R - AGCCGATCAGCCGCTACCTGTC	(Gupta et al., 2014; Karpinka et al., 2015)
sox9-enh	F - TGGCCTACAGAAAGGTGAG R - CGAGGCCAAGGACACCT	(Mead et al., 2013)
sox9-prom	F - CCTCACCTCTTCCAAATCG R - GCAGCATTAAATACCCTCCTC	(Ushita et al., 2014)
eef1a1o (positive control)	F - TATAGAACTGCCACAAGAAGCT R - CTACAAATGTGGTGGTATCGA	(Akkers et al., 2012)
tff2 (negative control)	F - CACACCGTTTGCCATTGTTT R - CATTTCCAACCTGGACTGAGTAA	(Akkers et al., 2012)

ChIP-qPCR primers (Mouse)

Gene	Sequence	Source
Eomes	F - GCCGCACATATATAAGCAGCC R - AGCAACCAGCCATTTCTCTC	(Kartikasari et al., 2013)

Foxa2	F- CACCTGGATTTGGGCCAACTA R-TTCTTGGTTCTGAAAATGTGACTAGG	(Kartikasari et al., 2013)
Pdx1	F - GAGAGCTCCACAGCAGCAAGC R - CCAGATCGCTTTGACAGTTCTCC	(Xu et al., 2011)
Sox9	F - CCCTTCCAAAATCCGGTCCA R - ACGTTAGATACCTCGGGCCA	(Ushita et al., 2014)

Table S2. List of primary antibodies for IF

Antibody	Raised in	Dilution	Source	Catalogue #
Setd7	Mouse	1:100	Abcam	ab14820
Pdx1	Rabbit	1:500	Abcam	ab47267
Foxa2	Rabbit	1:300	Abcam	ab40874
Insulin	Guinea Pig	1:250	Invitrogen	18-0067
E-cadherin	Rat	1:500	Invitrogen	13-1900
GM130	Mouse	1:250	BD Transd. Lab.	610823
Lamp1	Rabbit	1:50	Hybridoma Bank	553792

Table S3. List of antibodies for ChIP and IP/IB

Antibody	Raised in	Source	Catalogue #
Setd7	Rabbit	Biomol	A301-747A
Pol II	Rabbit	Diagenode	c15200004
Setd7	Mouse	Abcam	ab14820
H3K4me1	Rabbit	Abcam	ab8895
H3K4me3	Rabbit	Abcam	ab8580
H3K27ac	Rabbit	Abcam	ab4729
GFP	Rabbit	Abcam	ab290
Foxa2	Rabbit	Abcam	ab40874
Foxa2	Goat	Santa Cruz	sc-6554
Tubulin	Mouse	Sigma	T9026

SUPPLEMENTARY REFERENCES

Akkers, R., Jacobi, U. and Veenstra, G. (2012). Chromatin immunoprecipitation analysis of *Xenopus* embryos. *Methods Mol. Biol.* **917**, 279-292.

Blythe, S. A., Reid, C. D., Kessler, D. S., Klein, P.S. (2009) Chromatin Immunoprecipitation in Early *Xenopus* Laevis Embryos. *Dev Dyn.* **238**, 1422-1432.

Boyer, D., Fujitani, Y., Gannon, M., Powers, A., Stein, R. and Wright, C. (2006). Complementation rescue of *pdx1* null phenotype demonstrates distinct roles of proximal and distal cis-regulatory sequences in pancreatic and duodenal expression. *Dev. Biol.* **298**, 616–631.

Eisen J. S, Smith J. C. (2008) Controlling morpholino experiments: don't stop making antisense. *Development* **135**, 1735-43.

Gao, N., LeLay, J., Vatamaniuk, M. Z., Rieck, S., Friedman, J. R. and Kaestner, K. H. (2008). Dynamic regulation of *Pdx1* enhancers by *Foxa1* and *Foxa2* is essential for pancreas development. *Genes Dev.* **22**, 3435-3448.

Gerrish, K., Van Velkinburgh, J. and Stein, R. (2004). Conserved transcriptional regulatory domains of the *pdx-1* gene. *Molecular Endocrinology* **18**, 533–548.

Gupta, R., Wills, A., Ucar, D. and Baker, J. (2014). Developmental enhancers are marked independently of zygotic Nodal signals in *Xenopus*. *Dev. Biol.* **395**, 38-49.

Karpinka, J., Fortriede, J., Burns, K., James-Zorn, C., Ponferrada, V., Lee, J.,

Karimi, K., Zorn, A. and Peter D Vize, P. (2015). Xenbase, the *Xenopus* model organism database; new virtualized system, data types and genomes. *Nucleic Acids Res.* **43**, D756-763.

Kartikasari, A. E., Zhou, J. X., Kanji, M. S., Chan, D. N., Sinha, A., Grapin-Botton, A., Magnuson, M. A., Lowry, W. E. and Bhushan, A. (2013).

The histone demethylase *Jmjd3* sequentially associates with the transcription factors *Tbx3* and *Eomes* to drive endoderm differentiation. *EMBO J.* **32**, 1393-1408.

Mead, T., Wang, Q., Bhattaram, P., Dy, P., Afelik, S., Jensen, J. and Lefebvre,

V. (2013). A far-upstream (-70 kb) enhancer mediates *sox9* auto-regulation in somatic tissues during development and adult regeneration. *Nucleic Acids Res.* **41**, 4459–4469.

Nishioka, K., Chuikov, S., Sarma, K., Erdjument-Bromage, H., Allis, C. D.,

Tempst, P. and Reinberg, D. (2002). Set9, a novel histone H3 methyltransferase that facilitates transcription by precluding histone tail modifications required for heterochromatin formation. *Genes Dev.* **16**, 479-489.

Pashos, E., Park, J., Leach, S. and Fisher, S. (2013). Distinct enhancers of

ptf1a mediate specification and expansion of ventral pancreas in zebrafish. *Dev. Biol.* **381**, 471–481.

Rankin, S. A., Kormish, J., Kofron, M., Jegga, A. and Zorn, A. M. (2011). A gene regulatory network controlling *hhex* transcription in the anterior endoderm of the organizer. *Dev. Biol.* **351**, 297-310.

Tao, Y., Neppl, R. L., Huang, Z.-P., Chen, J., Tang, R.-H., Cao, R., Zhang, Y., Jin, S. W. and Wang, D. Z. (2011). The histone methyltransferase *Set7/9* promotes myoblast differentiation and myofibril assembly. *J. Cell Biol.* **194**, 551-565.

Ushita, M., Saito, T., Ikeda, T., Yano, F., Higashikawa, A., Ogata, N., Chung, U., Nakamura, K. and Kawaguchi, H. (2014). Transcriptional induction of *sox9* by NF-kappaB family member *rela* in chondrogenic cells. *Osteoarthritis and Cartilage* **17**, 1065–1075.

Wu, K., Gannon, M., PESHAVARIA, M., Offield, M., HENDERSON, E., Ray, M., Marks, A., Gamer, L., Wright, C. and Stein, R. (1997). Hepatocyte Nuclear Factor 3b Is Involved in Pancreatic beta-Cell-Specific Transcription of the *pdx-1* Gene. *Mol. Cell Biol.* **17**, 6002-6013.

Xu, C., Cole, P., Meyers, D., Kormish, J., Dent, S. and Zaret, K. (2011). Chromatin "prepattern" and histone modifiers in a fate choice for liver and pancreas. *Science* **332**, 963-966.